

# The unsteady Kármán problem for a dilute particle suspension

By M. R. FOSTER<sup>1</sup>, P. W. DUCK<sup>2</sup>  
AND R. E. HEWITT<sup>2</sup>

<sup>1</sup>Department of Aerospace Engineering and Aviation,  
The Ohio State University, Columbus, Ohio, 43210, USA

<sup>2</sup>Department of Mathematics, University of Manchester,  
Oxford Road, Manchester M13 9PL, UK

(Received 21 January 2001 and in revised form 25 July 2002)

We consider the unsteady three-dimensional Kármán flow induced by the impulsive rotation of an infinite rotating plane immersed in an incompressible viscous fluid with a dilute suspension of small solid monodisperse spherical particles. The flow is described in terms of a ‘dusty gas’ model, which treats the discrete phase (particles) and the continuous phase (fluid) as two continua occupying the same space and interacting through a Stokes drag mechanism. The model is extended to allow for a local gravitational acceleration in a direction parallel to the axis of rotation, and is valid for cases in which gravity acts either in the same direction as or in the opposite direction to the Ekman axial flow induced by the rotation of the plane.

Analysis based on the theory of characteristics shows that the role of gravity is crucial to the treatment of the discrete-phase equations, particularly in regard to the appropriate boundary conditions to be applied at the solid surface. Other notable features include the presence of an essential singularity in the solution when gravity is absent; indeed this phenomenon may help to explain some of the difficulties encountered in previous studies of this type. If the gravitational force is directed away from the rotating surface, a number of other interesting features arise, including the development of discontinuities in the particle distribution profiles, with corresponding particle-free regions contained between the interface and the rotating boundary. These ‘shock’ features can be associated with a critical axial location in the boundary layer at which a balance is achieved between Ekman suction induced by the rotating boundary and the influence of gravitational effects acting to move particles away from the boundary.

---

## 1. Introduction

The flow of a dispersed two-phase medium occurs in a large number of both environmental and industrial/technological contexts. It would clearly be invaluable to be able to model reliably the macroscopic behaviour of such flows, for example of dust/ash particles in environmental flows or micron-scale particulate matter in viscous fluids, such as contaminants in water treatment or efficiency-reducing particles in machinery oils. Similarly, many chemical processes often rely on two-phase flows involving the exposure of a large interfacial area through the use of dispersed particle clouds. In many of these cases, the fluid containing the particle load is also rapidly rotating, for example in separators, pumps and centrifuges. It is well known that

the global dynamics of such rotating flows are often driven by the properties of the contained three-dimensional boundary layers, which can lead to large-scale secondary flows, see for example Benton & Clark (1974) or Duck & Foster (2001).

In this work we apply analytical and computational methods to make predictions for complex particle-laden flows that can be subsequently tested experimentally. The modelling approach is based on the view that each material can be described as a continuum, occupying the same region in space. The significant feature of the model is that each of the interspersed media that form the 'mixture' can interact with the other through terms in the governing equations that correspond to inter-phase drag forces, as quantified through an associated particle Taylor number. For discussions of the theoretical approach to two-phase flows the reader is referred (for example) to the articles of Marble (1970), Ishii (1975), Drew (1983), Osipov (1997), Ungarish (1993), Jackson (1996), Zhang & Prosperetti (1997) and Hernández (2001).

The two phases to be considered here are a continuous fluid phase interspersed with a discrete solid particulate phase. The particles are taken to be small enough and of sufficient number to be treated as a continuum and allow concepts such as density and velocity to have physical meaning. The class of flows that we emphasize is the boundary layer induced above an infinite rotating plane immersed in an otherwise stationary dilute particle suspension; the term 'dilute' is used to indicate a volume fraction/particle concentration that is sufficiently small for the particle phase to be non-colloidal. There are clearly a broad range of physical effects that may be brought into a model of particle-laden flows; however, in this instance we introduce only the simplest formulation. In particular, we shall consider only the dilute limit for a solid monodisperse spherical particle phase. In doing so, we may formally neglect any effects related to phase transitions, non-uniformity of viscosity or deposition/friction at bounding surfaces and take the inter-phase momentum transfer to be due solely to a Stokes drag term for the spherical particles. Similarly, we shall assume that the particles are sufficiently large to ignore the effects of Brownian motion but sufficiently small to neglect Saffman (1965) and Magnus forces; we also assume that thermal effects and electrostatic forces are absent. The extension of the basic model to include these more general effects can be considered at a later stage. For validity of the two-phase model we shall require that the particles are much smaller than the natural lengthscale, which in this instance is the boundary-layer thickness.

The choice of the Kármán problem as a benchmark for the two-phase model is not only due to its inherent relevance to a range of applications, but also because it is 'exact' within the framework of the fluid-phase equations and is fully three-dimensional, thereby providing a stringent test (via relatively straightforward experimentation) for predictions of the macroscopic theory.

Additional motivation for an examination of the Kármán problem for a dilute suspension arises from its history in the literature. A first discussion of the problem was provided by Zung (1969), who utilized a formulation of the general type described by Marble (1970), but the analysis of Zung was controversial in some respects. A later discussion of the same problem was provided by Ungarish & Greenspan (1983) (hereafter referred to as UG), who identified some inconsistencies in the earlier work of Zung. Amongst these, are that Zung implicitly assumed that the particle concentration is constant across the boundary layer, and also that the numerical values of the parameters used in the computations correspond physically to particles of size comparable to the boundary layer (thereby being inconsistent with the assumptions of the macroscopic model).

Although it is clear that the points raised in UG noted above are valid, their other

objections to the analysis of Zung are less simply justified. In particular, there is an objection raised with regard to the absence of both pressure gradient forces and boundary conditions applied at the disk for the particle phase. Here we note that the aforementioned pressure gradient terms for the particulate phase are not universally adopted by all researchers in this field; however, their absence may be formalized by an assumption of a dusty-gas model in which the particulate phase has a large density relative to the surrounding fluid. Recent papers by Slater & Young (2001) and Hernández (2001) utilize equations without a particle pressure gradient. The inclusion of a particle viscosity may be an issue for general particle concentrations (if a correspondingly self-consistent theory can be developed for such cases); however, their inclusion in the dilute limit is also open to question. Nevertheless, even with the inclusion of pressure forces and viscous terms in the discrete-phase equations (thereby leading to essentially two coupled nonlinear Navier–Stokes-like systems) UG were still unable to provide convincing numerical solutions of the steady-state equations. In terms of the scaled boundary-layer coordinate, the domain over which a solution is to be sought to the boundary-layer equations must be semi-infinite, although clearly a truncation at some appropriate point is required in any numerical procedure. However, UG noted that their computations required the (theoretically semi-infinite) computational domain to be restricted to less than three non-dimensional boundary-layer units. For such a restrictive choice of domain truncation, solutions that are independent of the domain size were evidently not obtained. Further, difficulties at the boundary were avoided by the *ad hoc* introduction of a small suction or by the incorporation of a diffusive term in the continuity equation. We note that a subsequent unsteady evolution of the UG two-phase system proved equally problematic in the later work of Resnick (1990), in which the same *ad hoc* approach was required to obtain physically relevant results.

The later analysis of Allaham & Peddieson (1993) reconsidered the UG two-phase system of steady equations and discussed the features of the solution for a range of arbitrarily imposed boundary conditions applied on the particle phase at the disk. They consider two cases in particular, which correspond to no slip/penetration and ‘perfect’ slip/penetration conditions on the particulate phase. Allaham & Peddieson point out that in the absence of a ‘viscosity’ in the particle equations (that is, in the dusty-gas model), no solution could be found.

Hence, it appears that the question of what constitutes the proper model equations for a flow such as this is not yet fully resolved. Indeed, in what appears to be work done simultaneously, Jackson (1996) and Zhang & Prosperetti (1997) find that an averaging process leads to a much richer set of equations than any investigators seem to have used to date. The difficulty here, very well discussed by Jackson (1996), is that the averaging process, just as in Reynolds averaging for turbulent flow, always ends in the dilemma of closure of the system. So, it seems clear to us that an investigator ought to use the simplest set of equations that captures the new and major physics of the fluid–particle flow. That is the philosophy that underlies our approach in this work.

Nonetheless, there remain some difficulties in the application of the two-phase dusty-gas model to even the most simple of three-dimensional boundary-layer flows. In this paper we provide further details of the unsteady Kármán problem in an attempt to elucidate and resolve some of the difficulties that have been encountered so far in the existing literature. Additionally we incorporate the effects of a local gravitational acceleration into the model; as far as we are aware, such effects have not been studied in previous work of this type. As we shall show, the inclusion of

gravitational effects leads to some interesting effects and also helps to clarify the gravity-free case.

The format of the paper is as follows. In §2, we formulate the two-phase model in the limit of a dilute suspension, giving details of the conditions applied at the disk. In §3, some flow properties at the disk surface are deduced. In §4, the limiting solutions for a large particle Taylor number are considered both with and without the effects of gravity (an analysis of the short-time behaviour of the solutions is given in Appendix B), and finally in §5 we provide some conclusions and general discussion.

## 2. Formulation

The notional configuration under consideration here is depicted in figure 1. A container of an incompressible fluid interspersed with a solid particulate phase is spun up from a state of rest. In this initial work we consider only the dynamics of the boundary layers that form on the upper and lower horizontal bounding surfaces, neglecting the influence of the sidewalls, and seeking a radially self-similar flow of von Kármán form. In terms of the physical situation illustrated by the figure, we may expect such a solution to describe the flow response over an order-one dimensionless timescale non-dimensionalized with respect to the angular frequency  $\Omega$ . These boundary layers are known to be the crucial driving mechanism for the spin-up process, and (see for example Duck & Foster 2001) in the case of a single-phase fluid, are fully developed within one rotation of the container. Over a much longer dimensionless timescale of  $O(E^{-1/2})$ , where  $E = \Omega H^2/\nu \ll 1$ , based on the container height  $H$  and kinematic viscosity  $\nu$ , recirculation driven by these viscous layers will significantly influence the interior flow.

In our theoretical model we therefore consider an (infinite) incompressible fluid body, interspersed with a suspension of particles (of uniform size and density), above a plane that is impulsively spun up from a state of rest. Since we consider our fluid to be bounded by two horizontal planes, we shall in essence consider three broad classes of problem. The three classes correspond to no gravitational influence, a gravitational acceleration towards the boundary (e.g. for the lower boundary layer in figure 1) and a gravitational acceleration away from the boundary (e.g. for the upper boundary layer in figure 1). (This configuration should be considered as conceptual, rather than precise, since the global flow will not be addressed; rather we consider each boundary layer in isolation over a timescale for which the interior flow is unchanged.) As we shall see below, these three cases will be distinguished as  $\mathcal{K} = 0$ ,  $\mathcal{K} > 0$  and  $\mathcal{K} < 0$  respectively, where  $\mathcal{K}$  is a dimensionless parameter (defined precisely below) that measures the relative importance of rotational and gravitational effects.

Assuming that the particle suspension is dilute, the continuity equations for the fluid and the suspension are taken to be

$$\nabla \cdot \mathbf{u} = 0, \quad \frac{\partial \alpha}{\partial t^*} + \nabla \cdot (\alpha \mathbf{u}_p) = 0, \quad (2.1a, b)$$

where  $\mathbf{u}$  is the velocity vector of the fluid component,  $\mathbf{u}_p$  is the velocity vector of the particle phase,  $\alpha$  is the particle concentration of the particle phase and  $t^*$  is a dimensional time. The momentum equations for the two phases are taken to be

$$\rho_f \frac{\partial \mathbf{u}}{\partial t^*} + \rho_f (\mathbf{u} \cdot \nabla) \mathbf{u} + \nabla p = \mu \nabla^2 \mathbf{u} - \mathbf{F} - \rho_f \mathbf{g}, \quad (2.2a)$$

$$\rho_p \alpha \frac{\partial \mathbf{u}_p}{\partial t^*} + \rho_p \alpha (\mathbf{u}_p \cdot \nabla) \mathbf{u}_p = \mathbf{F} - \rho_p \alpha \mathbf{g} + \rho_f \alpha \mathbf{g}, \quad (2.2b)$$

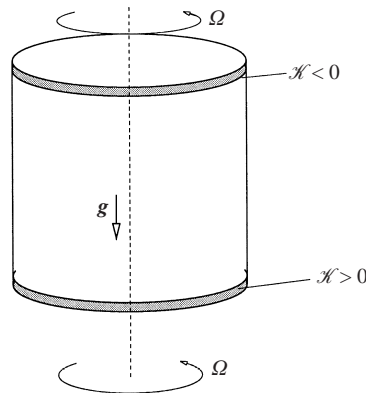


FIGURE 1. Configuration of a spin-up problem, showing a boundary layer under the top boundary, for which  $\mathcal{K} < 0$ ; and one over the bottom boundary, for which  $\mathcal{K} > 0$ .

where a buoyancy term has been included as well as the standard gravitational force. In these equations,  $\rho_f$  and  $\rho_p$  denote the (constant) densities of the fluid and particle phases respectively, whilst  $\mathbf{g}$  is the local gravitational acceleration, which is taken to be parallel to the axis of rotation of the infinite rotating plane. These equations are the so-called ‘dusty-gas’ equations of many authors, and a discussion of their domain of validity is given below.

Completion of these equations requires that the drag force per unit volume  $\mathbf{F}$ , between the two species be specified. In our case, following previous studies of this type, we assume small spherical particles, and so we apply the Stokes drag formula

$$\mathbf{F} = \frac{9\mu}{2a^2}\alpha(\mathbf{u} - \mathbf{u}_p), \tag{2.3}$$

where  $a$  is a particle diameter. This Stokes drag formula assumes that  $\alpha$  is sufficiently small for the particles to be non-interacting, and consistent with this assumption of negligible particle–particle collisions, there is no ‘viscosity’ in the particle phase described by equation (2.2*b*).

Two fluid/particle parameters are crucial to the modelling that follows. The parameter  $\gamma \equiv \rho_p/\rho_f$  obviously measures the relative densities of the particle material and the fluid. The ratio of the Stokes drag term in (2.2*a*) to the fluid inertia is  $\alpha\beta$ , where  $\beta \equiv 9\nu/(2\Omega a^2)$  is an inverse particle Taylor number. (Here,  $\nu = \mu/\rho_f$  is the kinematic viscosity for the fluid.) For small particles,  $\beta$  is typically very large.

### 2.1. Parametric restrictions

Equations (2.1)–(2.2*b*) are not the most general two-fluid equations for such a flow. Zhang & Prosperetti (1997) and Jackson (1996) indicate that several additional terms, including viscous stresses and ‘Reynolds stresses’ may, in general, be present. The question of just what equations are in fact appropriate is related to the relative orders of  $\alpha$ , and parameters  $\gamma$  and  $\beta$ .

To be more specific, the more general form of (2.1*a*) is given by Jackson (1996) or Ungarish (1993) (for example). However, we assume that  $\alpha$  is so small that it may be neglected compared to 1 in the first term, and also that  $\alpha|\mathbf{u}_p| \ll |\mathbf{u}|$  everywhere in the flow, which permits the use of (2.1). This assumption must be checked *a posteriori*. We return to this in §2.4. Further, in equation (2.2*a*), a factor  $(1 - \alpha)$  multiplies

the pressure gradient term and the inertia term. Again, consistent with the small- $\alpha$  requirement for a dilute medium, all of those factors have been replaced by 1.

Finally, in equation (2.2*b*), all references noted above and in the introduction indicate the presence of a term

$$\frac{1}{\gamma} \nabla p.$$

Provided that  $\gamma$  is sufficiently large, this effect can be neglected as well. Again, we make an *a posteriori* check in §2.4. In addition, consistent with the small- $\alpha$  requirement, the viscosity in (2.2*a*) does not have the Einstein correction.

We have retained the Stokes drag in (2.2*a*) and (2.2*b*) even though it has an  $\alpha$  multiplier—this is self-consistent only if its multiplier,  $\beta$ , is large—a requirement which we now invoke. Having already required that the ratio  $\gamma \equiv \rho_p/\rho_f$  be large, these restrictions together lead to the equation set (2.1)–(2.2*b*) for a ‘dusty-gas’ (Marble 1970). This same set of approximations has been widely used in the literature, most recently, for example, in the papers by Slater & Young (2001) and Hernández (2001). The assumptions are further discussed at a more fundamental level by Jackson (1996). Again, we return to a reassessment of this matter in §2.4.

In summary, then, the parametric restrictions to this point are

$$\alpha \ll 1, \quad \beta \gg 1, \quad \gamma \gg 1. \quad (2.4)$$

Typically, in multi-parameter problems of this sort, certain more restrictive relative orderings among  $\alpha, \beta$  and  $\gamma$  can be expected to develop; such more stringent restrictions will be noted as they arise in the course of the analysis. However, for the sake of completeness, we note here that all of what we do here also requires

$$\beta \gg \gamma. \quad (2.5)$$

Furthermore, asymptotic analysis of the no-gravity solution structure in §4.1.1 leads to a yet more severe restriction for that case, given in (4.18), which is

$$\gamma^2 \gg \beta \gg \gamma \gg 1 \quad \text{for} \quad \mathcal{K} = 0. \quad (2.6)$$

## 2.2. Self-similar equations

We consider a cylindrical polar coordinate system  $(r, \theta, z)$  centred on the axis of rotation with the plane  $z = 0$  being the impermeable boundary. The boundary layer on the lower surface is assumed to develop in time according to the self-similar structure

$$\mathbf{u} = (\hat{u}, \hat{v}, \hat{w})^T, \quad \mathbf{u}_p = (\hat{u}_p, \hat{v}_p, \hat{w}_p)^T, \quad (2.7)$$

where

$$\hat{u} = \Omega r u(\zeta, t), \quad \hat{v} = \Omega r v(\zeta, t), \quad \hat{w} = (v\Omega)^{1/2} w(\zeta, t), \quad (2.8)$$

$$\hat{u}_p = \Omega r u_p(\zeta, t), \quad \hat{v}_p = \Omega r v_p(\zeta, t), \quad \hat{w}_p = (v\Omega)^{1/2} w_p(\zeta, t), \quad (2.9)$$

$\zeta$  is the ‘boundary-layer’† variable  $\zeta \equiv z(\Omega/\nu)^{1/2}$ , and the kinematic viscosity is based on the fluid density as above. Non-dimensional time is taken to be  $t = \Omega t^*$  and the vector  $\mathbf{r}$  is in the radial direction. Note that the particle concentration,  $\alpha$ , is also a function of  $\zeta$  and  $t$ .

† Although there is no formal boundary-layer approximation required for an infinite geometry, we shall still refer to the region as the boundary layer for convenience.

Substitution of these quantities into equations (2.1)–(2.2b) leads to

$$\dot{u} + wu' + u^2 - v^2 = u'' - \beta\alpha(u - u_p), \tag{2.10}$$

$$\dot{v} + wv' + 2uv = v'' - \beta\alpha(v - v_p), \tag{2.11}$$

$$\dot{u}_p + w_p u'_p + u_p^2 - v_p^2 = \frac{\beta}{\gamma}(u - u_p), \tag{2.12}$$

$$\dot{v}_p + w_p v'_p + 2u_p v_p = \frac{\beta}{\gamma}(v - v_p), \tag{2.13}$$

$$2u + w' = 0, \tag{2.14}$$

$$\dot{\alpha} + w_p \alpha' + \alpha(2u_p + w'_p) = 0, \tag{2.15}$$

where the prime denotes differentiation with respect to  $\zeta$  and the dot notation denotes differentiation with respect to non-dimensional time. The vertical component of (2.2b) remains coupled to the above system and must be incorporated, namely,

$$\dot{w}_p + w_p w'_p = \frac{\beta}{\gamma}(w - w_p) - \mathcal{K}. \tag{2.16}$$

It is the assumption that  $\gamma \gg 1$  that leads to (2.16), with the terms shown dominating the neglected pressure gradient term. Indeed, this equation plays a crucial role in our analysis, insofar as it closes our model, effectively providing an explicit means to determine the particle velocity component  $w_p$ . The quantity  $\mathcal{K} \equiv (1 - \gamma^{-1})g/\sqrt{v\Omega^3}$  is a gravitational parameter that measures the net buoyancy in the flow, which is zero in the absence of gravity. Since  $\gamma$  is large, the buoyancy force *per se* is negligible, and all that matters is gravity acting on the particles themselves. The vertical component of the fluid momentum equation (2.2a) takes its usual form in boundary-layer theory,  $\partial p/\partial \zeta = 0$ , leading then to no radial pressure gradient in this problem.

If we repeat the above analysis for the boundary layer under the top surface, writing instead  $\zeta = (h - z)(\Omega/v)^{1/2}$ , similar equations develop, which reduce to the set given above under the transformation  $(w, w_p, \mathcal{K}) \rightarrow (-w, -w_p, -\mathcal{K})$ . Therefore, studying (2.10)–(2.16) as written corresponds to the boundary layer on the lower wall for  $\mathcal{K} > 0$ , and to that on the upper wall for  $\mathcal{K} < 0$ . What is significant, from the point of view of the dynamics of the boundary layer, is that in one case the particle gravitational force is directed toward the wall ( $\mathcal{K} > 0$ ), and in the other case, away from the wall ( $\mathcal{K} < 0$ ).

In this paper we will explore the dependence of the solutions on the various parameters,  $\gamma$ ,  $\beta$  and  $\mathcal{K}$ . Note that  $\beta^{1/2} \sim (v/\Omega)^{1/2}/a$  is the ratio of the boundary-layer thickness to the particle size, which clearly must be large to support a continuum hypothesis, thus lending support to one of the restrictions in (2.4). The quantity  $\mathcal{K}$  could be numerically small in some industrial settings, where the rotation rate is high; in the context of many laboratory experiments however, the rotation rates are sufficiently small for  $|\mathcal{K}|$  to be large.

### 2.3. Boundary and initial conditions

For the ‘dusty-gas’ boundary layer under study here, we suppose that the fluid satisfies impermeability and no slip, but that the particles can be allowed to slip at the surface (there being no ‘particle viscosity’), hence we have the boundary conditions

$$u = w = 0, \quad v = 1 \quad \text{at} \quad \zeta = 0, \tag{2.17}$$

and

$$u, v, u_p, v_p \rightarrow 0 \quad \text{as } \zeta \rightarrow \infty, \quad (2.18)$$

together with the condition that the particle concentration matches to that in the interior,

$$\alpha \rightarrow \alpha_e \quad \text{as } \zeta \rightarrow \infty. \quad (2.19)$$

The proper condition to be imposed on  $w_p$  at the boundary is not immediately apparent. At first, it would appear that a non-penetration condition,

$$w_p = 0 \quad \text{at } \zeta = 0, \quad (2.20)$$

is appropriate, and this constraint is in fact often used in the literature. However, it is evident from (2.16) that if  $w_p > 0$  near the wall, then the variable  $\zeta$  is time-like (that is, the  $\zeta, t$  characteristics slope away from the wall), and it is certainly mathematically correct to set  $w_p$  to zero, or indeed any value, at the wall. It is conceivable that a model could be constructed to incorporate the particle-wall interactions, for example simulating bouncing and including coefficients of restitution etc., but this is considered to be outside the scope of the present paper. Indeed, great difficulties can arise in such circumstances due to the possibility of crossing particle trajectories; this and other issues are discussed by Osipov (1997) and Slater & Young (2001).

If  $w_p < 0$  near the wall, then the  $\zeta, t$  characteristics of (2.16) slope toward the wall, and so  $w_p$  cannot properly be specified there, but must rather be specified elsewhere, for example at the edge of the layer. We return to this question subsequently, since this has important implications for both the physics and computations in some parameter regimes.

In essence, the physical interpretation is simple. If there is a net axial flow of particles towards the boundary, the properties of this particle phase at the boundary are obtained as part of the solution procedure and cannot in general be specified. For the converse case, if the net transport is away from the boundary, one is free to impose any conditions at the wall and the influence of such conditions propagates outwards through the boundary layer. The somewhat more complex situation for which the axial transport of particles changes at a location within the boundary layer will be discussed later.

The question of initial conditions ought to reflect what is physically realistic for a laboratory investigation, and so we consider an initial state of uniform ‘settling’ of the particles under gravity, namely

$$\alpha = \alpha_i(\zeta), \quad w_p = -\gamma \mathcal{K} / \beta \quad \text{at } t = 0. \quad (2.21)$$

Generally we take  $\alpha_i(\zeta) = \alpha_e$  uniform, unless otherwise stated. The fluid velocity components are all taken to be zero at  $t = 0$ , corresponding to spin-up of the fluid from rest.

#### 2.4. Further comments on the dusty-gas approximation

We set out above an approximate set of equations under the assumptions discussed in §2.1. We here return to those approximations for further analysis for the special case of this self-similar boundary layer.

##### *The pressure term*

As noted in the discussion in §2.2, the leading-order pressure gradient across the boundary layer is zero. There is, of course, a smaller pressure change, and writing the



reduced pressure as  $p = \rho_f \nu \Omega \hat{p}$  and inserting into the vertical component of the fluid momentum equation (2.2a) gives the following equation:

$$\dot{w} + ww' + \hat{p}' = w'' - \alpha\beta(w - w_p). \tag{2.22}$$

Similarly, substituting into the vertical component of (2.2b), whilst retaining the (previously neglected) pressure term gives the equation

$$\dot{w}_p + w_p w_p' + \frac{1}{\gamma} \hat{p}' = -K + \frac{\beta}{\gamma}(w - w_p). \tag{2.23}$$

Elimination of  $\hat{p}'$  from these two equations gives, after again neglecting  $\alpha$  when it occurs in the combination  $(1 + \alpha)$ ,

$$\dot{w}_p + w_p w_p' + \frac{\beta}{\gamma} w_p = \frac{1}{\gamma} (\dot{w} + ww' - w'') + \frac{\beta}{\gamma} w - \mathcal{K}. \tag{2.24}$$

This equation suggests that relatively complicated asymptotic expansions exist for the vertical velocity components, in the case  $\mathcal{K} \equiv 0$ . The expansions are

$$\begin{pmatrix} w \\ w_p \end{pmatrix} = \begin{pmatrix} w_0 \\ w_{p0} \end{pmatrix} + \frac{\gamma}{\beta} \begin{pmatrix} w_1 \\ w_{p1} \end{pmatrix} + \dots + \frac{1}{\gamma} \begin{pmatrix} w_\gamma \\ w_{p\gamma} \end{pmatrix} + \dots, \tag{2.25}$$

where the form of the series is governed by the constraint (2.6). The gauge functions beyond the first two terms are dependent on the relative orders of  $\beta$  and  $\gamma$ , even under (2.6). Superficially it may appear that the solutions we have obtained for the leading-order terms in this series are not uniformly valid to the wall, specifically the  $\gamma^{-1}$  term; however, a careful inspection of the heirarchy of equations generated by the series reveals that the  $\gamma^{-1}$  term is dependent on those terms that precede it in the asymptotic series. Thus, beyond the first two terms, it is difficult to say much about the higher-order terms in the series, and the first two terms are those that arise from the subset equation (2.16). In fact, neglect of the  $\gamma^{-1}$  term is self-consistent. It may be that there is a higher-order non-uniformity, but it would be ill-advised to draw such a conclusion based on arguments from the  $(w, w_p)$  equations only, since such a complex asymptotic expansion (2.25) must be inserted into the complete equations, and would require retaining terms already neglected, as noted.

On the other hand, for  $\mathcal{K} \neq 0$ , one can observe from this equation that retention of the gravity term requires its largeness compared to  $\gamma^{-1}$ , so  $\gamma \gg 1$  is not sufficient in this case, but rather

$$\gamma \gg \mathcal{K}^{-1} \quad \text{for } \mathcal{K} \neq 0. \tag{2.26}$$

*Continuity*

The approximate continuity equation (2.14) results from what may be regarded as a regular perturbation in a small parameter measuring the magnitude of  $\alpha$  (for example  $\alpha_c$ ), although (more precisely) the procedure adopted is much like a Boussinesq approximation: we neglect  $\alpha$  everywhere except when it is multiplied by the (assumed large)  $\beta$ , and we neglect  $\gamma^{-1}$  except when it is multiplied by  $\beta$ . That is a self-consistent approximation, provided that (2.26) is satisfied in the presence of gravitational force.

**3. Numerical solution**

The numerical method is based on a Crank–Nicolson scheme temporally, standard second-order central differencing in  $\zeta$ , with Newton iteration to handle the inherent

nonlinearity of the system. The net result is a banded algebraic system (at each timestep, at each iteration level), whose structure is fully exploited in the solution procedure. Our early numerical investigations identified some subtleties with regard to the appropriate formulation of boundary conditions for the particle-phase velocity components and  $\alpha$ . However, in the light of the preceding comments regarding the  $\zeta - t$  characteristics near the wall, and a more detailed analysis to be presented in subsequent sections, we are able to fully justify the appropriate choices of boundary condition used in the numerical procedure.

For a boundary layer in which  $\mathcal{K} > 0$  (see figure 1), since (as noted earlier) the characteristics of the particle equations are directed towards  $\zeta = 0$ , it is therefore entirely appropriate to specify particle-phase flow quantities as  $\zeta \rightarrow \infty$ , and to determine these quantities on the disk surface as part of the solution procedure. This procedure leads to fully consistent numerical solutions.

In the case that  $\mathcal{K} < 0$  (see figure 1) the characteristics of the particle-phase equations are generally directed outwards, away from the boundary at  $\zeta = 0$ , suggesting the appropriate (numerical) procedure is to specify  $u_p$ ,  $v_p$ ,  $w_p$  and  $\alpha$  on the disk surface, whilst as  $\zeta \rightarrow \infty$ , to retain the use of (2.12), (2.13), (2.15), (2.16) but impose a uniform behaviour in the far field, with  $\partial u_p / \partial \zeta = \partial v_p / \partial \zeta = \partial w_p / \partial \zeta = \partial \alpha / \partial \zeta = 0$  as  $\zeta \rightarrow \infty$ ; again, this procedure leads to consistent numerical solutions. In the no-gravity case ( $\mathcal{K} = 0$ ) either of the aforementioned procedures was seen to yield consistent numerical results (and indeed the two approaches produce solutions that agree in this case).

We begin the presentation of the numerical results by noting that, without loss of generality, we may perform the computations for varying  $\alpha_e$ ,  $\beta$  and  $\mathcal{K}$  with  $\gamma$  fixed, since the crucial parameters are in fact  $\alpha\gamma$ ,  $\beta/\gamma$  and  $\mathcal{K}$ . Results of the time integration of the initial-boundary-value problem formed by (2.10)–(2.16) are shown in figures 2–8, and are described next.

#### *Flow with negligible gravity: $\mathcal{K} \approx 0$*

In figures 2 and 3 we present examples of the radial fluid and particle velocity components with increasing time for  $\beta/\gamma = 10$  and  $\alpha_e\gamma = 0.1$ . Figure 2 shows a slip velocity for the particle phase at the surface of the disk, which is in agreement with the results of Appendix A, detailing the time evolution of surface conditions. Figure 3 shows profiles of the particle concentration for the same time evolution, showing the development of a ‘low- $\alpha$ ’ region immediately adjacent to the disk. This may be expected on physical grounds since the disk acts like a centrifugal fan, ejecting fluid radially outwards with a corresponding axial mass replacement. However, impermeability of the disk and the absence of gravity suggests that a replacement mechanism for the particle phase does not exist near to the disk. The exponential behaviour of the particle concentration at the surface is again in agreement with the analysis of Appendix A. It is interesting to note the behaviour near the wall, where it appears that  $\alpha \rightarrow 0$  over a finite zone. At the maximum time shown,  $t = 20$ , the velocity components are essentially steady, but  $\alpha$  in the near-wall region is still noticeably evolving toward zero.

The velocity profiles shown here are, at first sight, qualitatively similar to those shown in Ungarish (1993) as computed from a broader class of model equations by Resnick (1990). The volume-fraction profile is also similar, with the ‘width’  $\zeta \sim 1$  for both. However, we must note that differences still exist. For example, the profiles of figure 5.4.3 in Ungarish (1993) for the difference in axial velocity between the two phases change sign, leading to a region of the flow in which particles move against the

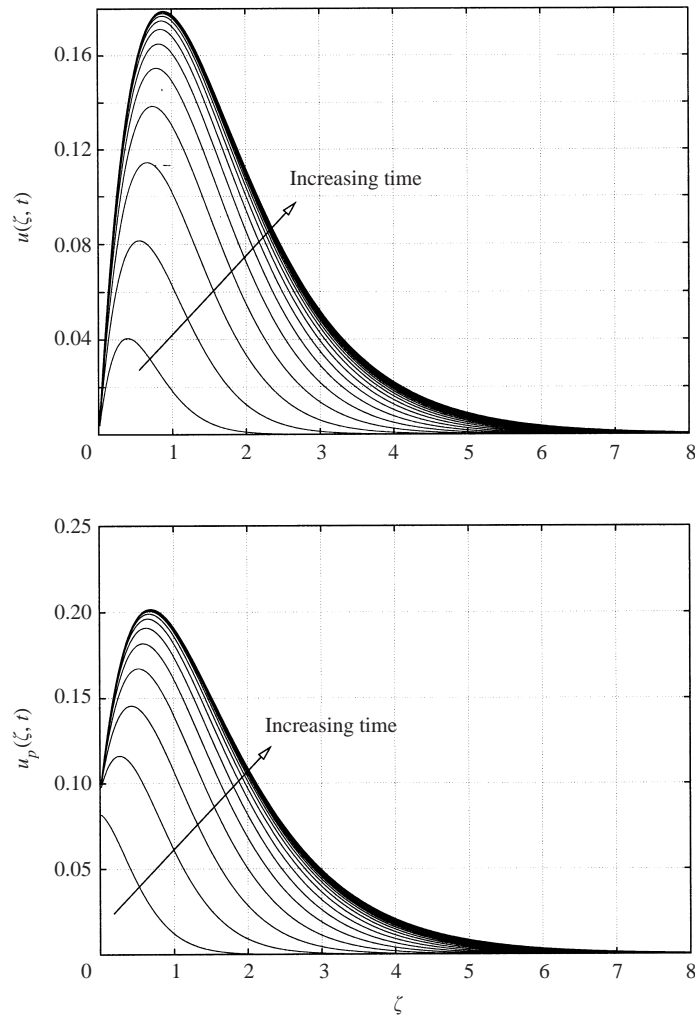


FIGURE 2. Profiles of the fluid and particle-phase radial (dimensionless) velocity for  $\alpha_e\gamma = 0.1$ ,  $\beta/\gamma = 10$  and  $\mathcal{K} = 0$  at  $t = 0.5, 1, \dots, 20$ .

dominant Ekman transport; this is in qualitative contrast to our results of figure 6 in the large-time limit. We may further note that the unsteady results described by Ungarish (1993) still use the *ad hoc* suction boundary condition to avoid difficulties with application of the no-penetration condition; the same review also notes that the unsteady numerics lead to the volume fraction reaching ‘non-physical values’ in the large-time limit, again in contrast to our own theory.

Figure 4 shows the evolution of the particle velocity components at the wall, for  $\beta/\gamma = 10$ . Clearly, the radial slip velocity of the particle phase,  $u_{po} \equiv u_p(\zeta = 0, t)$  (the additional zero subscript here denotes an evaluation of the quantity at the disk surface,  $\zeta = 0$ ) approaches a positive limiting value, as does  $v_{po} \equiv v_p(\zeta = 0, t)$ , consistent with the concepts of the phase-plane analysis of Appendix A. In figure 5, it is evident that, on a much longer timescale (because  $u_{po}$  is small), the particle concentration  $\alpha \rightarrow 0$  at the disk surface. This is again in excellent quantitative agreement with the results of the analysis of Appendix A, in particular with (A 13).

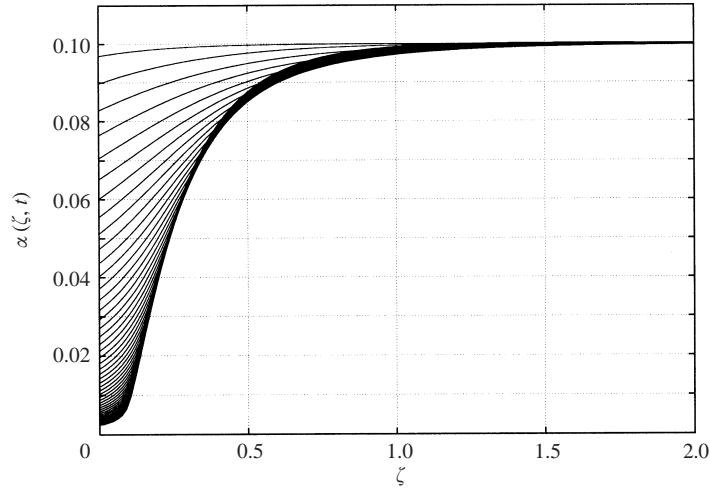


FIGURE 3. Profiles of the particle concentration for  $\alpha_e\gamma = 0.1$ ,  $\beta/\gamma = 10$  and  $\mathcal{K} = 0$  at  $t = 0.5, 1, \dots, 20$ .

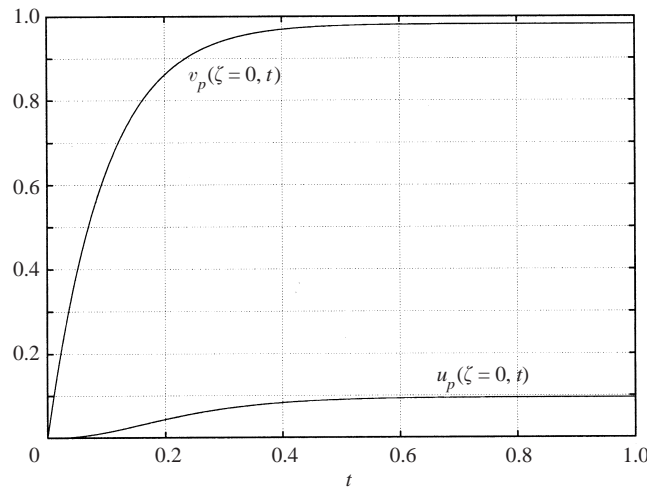


FIGURE 4. Horizontal velocity components at the wall for  $\alpha_e\gamma = 0.1$ ,  $\beta/\gamma = 10$  and  $\mathcal{K} = 0$ .

It is immediately evident from (A 3) and (A 6) that at larger values of  $\beta$  there is a strong scale separation. Provided that (A 7) is not satisfied, so that a finite-time singularity does not arise, then  $A = w'_p(\zeta = 0) \rightarrow 0$  on a very short scale, a time of  $O(\gamma/\beta)$ . However, the particle concentration at the wall,  $\alpha_o \equiv \alpha(\zeta = 0, t)$ , decays exponentially but very slowly, on a scale of order  $\beta/\gamma$ . In fact, for large  $\beta$ , the approximate solution of (A 3) is

$$\alpha_o \sim \alpha_i e^{-2\gamma t/\beta}, \tag{3.1}$$

since, from (A 9), the approximate value of  $u_{po}$  for large  $\beta$  is  $\gamma/\beta$ .

In figure 6, we present details for a case at higher particle Taylor number,  $\beta/\gamma = 50$ , with an interior particle concentration satisfying  $\alpha_e\gamma = 0.01$  and no gravitational effects ( $\mathcal{K} = 0$ ). The figure shows profiles of relative axial velocity between the two phases. As seen explicitly from the small-time analysis of Appendix A, far from the disk

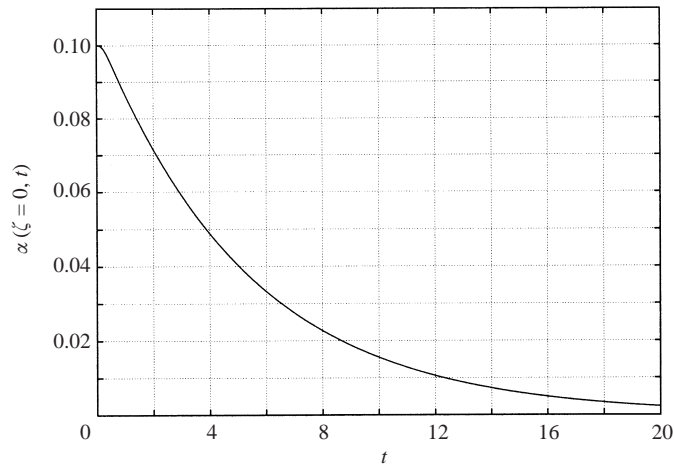


FIGURE 5. Particle concentration at the wall for  $\alpha_e\gamma = 0.1$ ,  $\beta/\gamma = 10$  and  $\mathcal{K} = 0$ .

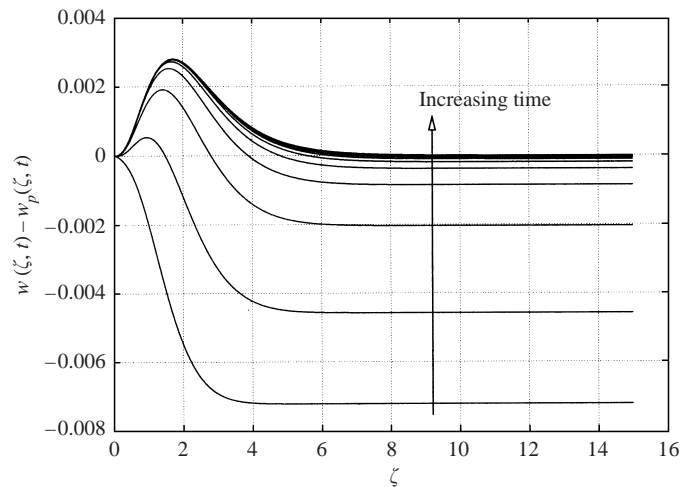


FIGURE 6. Profiles of the relative fluid/particle axial velocity for  $\alpha_e\gamma = 0.01$ ,  $\beta/\gamma = 50$  and  $\mathcal{K} = 0$  at  $t = 1, \dots, 20$ .

surface the axial components differ initially; however, in the large-time limit there is little relative axial velocity between the two phases in this zone.

It is well known that the sudden rotation of a boundary in an otherwise stationary fluid produces a resultant flow in the manner of a centrifugal fan, with a radial transport of fluid and concomitant axial flow towards the rotating boundary required to satisfy mass conservation. The relative directions of the gravitational forcing and this induced axial flow (or Ekman mass transport, as it is commonly referred to) is crucial for the qualitative behaviour of the flow.

*Gravitational acceleration directed towards the boundary:  $\mathcal{K} > 0$*

In figures 7 and 8 we show results that explore the case  $\mathcal{K} > 0$ , that is when the influence of a gravitational forcing is directed in the same sense as the Ekman mass transport. In figure 7, the behaviour of the particle concentration at the wall is shown for  $\beta/\gamma = 50$ ,  $\alpha_e\gamma = 0.01$ , for varying  $\mathcal{K} = 0, 10, 50, 100$ . In general, for  $\mathcal{K} > 0$ ,

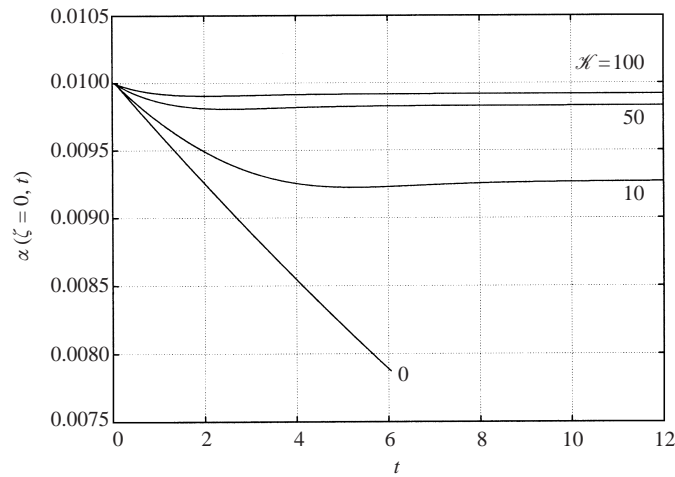


FIGURE 7. Behaviour of the particle concentration at the wall for varying gravitational influence with  $\alpha_e\gamma = 0.01$ ,  $\beta/\gamma = 50$ .

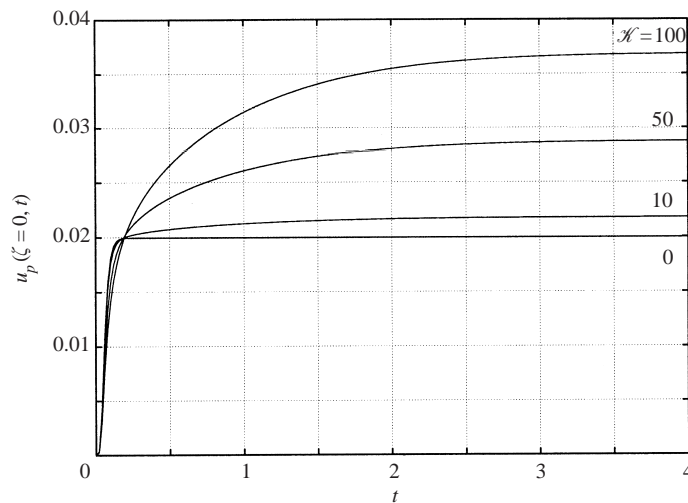


FIGURE 8. Particle slip velocity (in the radial direction) at the wall for varying gravitational influence with  $\alpha_e\gamma = 0.01$ ,  $\beta/\gamma = 50$ .

gravity provides a replacement mechanism for particles in the near-wall region, and typically the particle concentration at the wall is seen to reduce slightly to a minimum (due to the induced radial outflow subsequent to rotation of the boundary) before increasing again towards an eventual steady state. The timescale for the attainment of a steady behaviour is seen to be of the order of one rotation of the tank, and the scale separation observed in the absence of gravity (noted above) no longer holds.

We note that in the case  $\mathcal{K} > 0$  we have been able to solve the steady governing equations via a numerical approach directly (rather than as the large-time solution in an initial-value formulation); the states obtained from this solution procedure coincide with those obtained in the large-time limit of the unsteady calculations, as expected. However, in the limit  $\mathcal{K} \rightarrow 0^+$  it became increasingly difficult to obtain

converged numerical solutions to the steady equations. Such difficulties have been encountered (but not resolved) by previous authors seeking numerical solutions to the steady equations in the absence of gravity, for example by UG. The property of the solution structure that leads to these difficulties (an essential singularity) for  $\mathcal{K} = 0$  will be described in some detail subsequently (in §4), by considering the asymptotic limit of  $\beta \gg 1$ .

*Gravitational acceleration directed away from the boundary:  $\mathcal{K} < 0$*

In this case it may be anticipated that there exists the possibility of a qualitatively different flow evolution caused by the introduction of two competing effects. Clearly, the rotation of the disk induces an axial (Ekman) transport in the fluid as in the classical problem of von Kármán. However, there is an opposing influence of gravitational effects exerted on the particles that causes a uniform motion in the absence of any fluid motion. It is possible that the two effects of the Stokes drag induced by the non-uniform Ekman suction in the boundary layer and the uniform gravitational forcing may balance at a critical location within the layer. At  $\zeta$  locations beneath this critical location, gravitational effects dominate and particles will move away from the boundary, whilst at  $\zeta$  locations above this level, drag forces dominate and the Ekman mass transport is sufficient to induce a motion towards the boundary. Clearly, there is still radial transport since the flow is three-dimensional, but particles can be replenished from the interior flow provided that  $\alpha_e \neq 0$ .

The imposition of the initial conditions implemented above must lead, inevitably, to discontinuities in the particle concentration function (changing from  $\alpha(\zeta = 0, t = 0-) = \alpha_e$  at the wall, to, instantaneously  $\alpha(\zeta = 0, t = 0+) = 0$ ), which leads to the associated difficulties with computations of this type. Instead (and this in many respects turns out to be more revealing) we decided to perform  $\mathcal{K} < 0$  computations with an initial continuous, but non-uniform, spatial distribution of particles that are moving uniformly under gravity at a terminal velocity with  $w_p = -\gamma\mathcal{K}/\beta$ , an example of which is shown in figure 9. As in the preceding calculations, at time  $t = 0$  the disk is set to rotate at a unit non-dimensional angular frequency. (These initial conditions mirror what one may expect to achieve in a straightforward laboratory investigation.) As can be observed from the figure, the large-time structure includes the development of a shock-like profile in the distribution of the particle concentration. This developing discontinuity bounds a particle-free region ('below') and is located at a critical point at which there is no axial flow ( $w_p = 0$ ) of the discrete phase. Examination of the other velocity components indicates that a continuous distribution is obtained for  $u, v, w, u_p, v_p$  and  $w_p$ .

We note that the development of a discontinuity in the particle concentration relies upon striking a balance between drag forces exerted by the axial Ekman transport and gravitational effects. Therefore, if the influence of gravity is sufficiently strong (i.e.  $\mathcal{K} < \mathcal{K}_{crit} < 0$ ) then Ekman transport (and associated Stokes drag exerted on the particle phase) can be too weak to produce a shock and any distribution of particles ultimately rises away from the disk to infinity. In such a case, a steady-state cannot exist. This is precisely what occurs in the large-negative- $\mathcal{K}$  asymptotic solution given below in §4.3.1.

Development of such shocks has been mentioned by a variety of investigators previously, as noted by UG, Ungarish (1993), and also in a recent interesting paper by Mang, Ungarish & Schaffinger (2001).

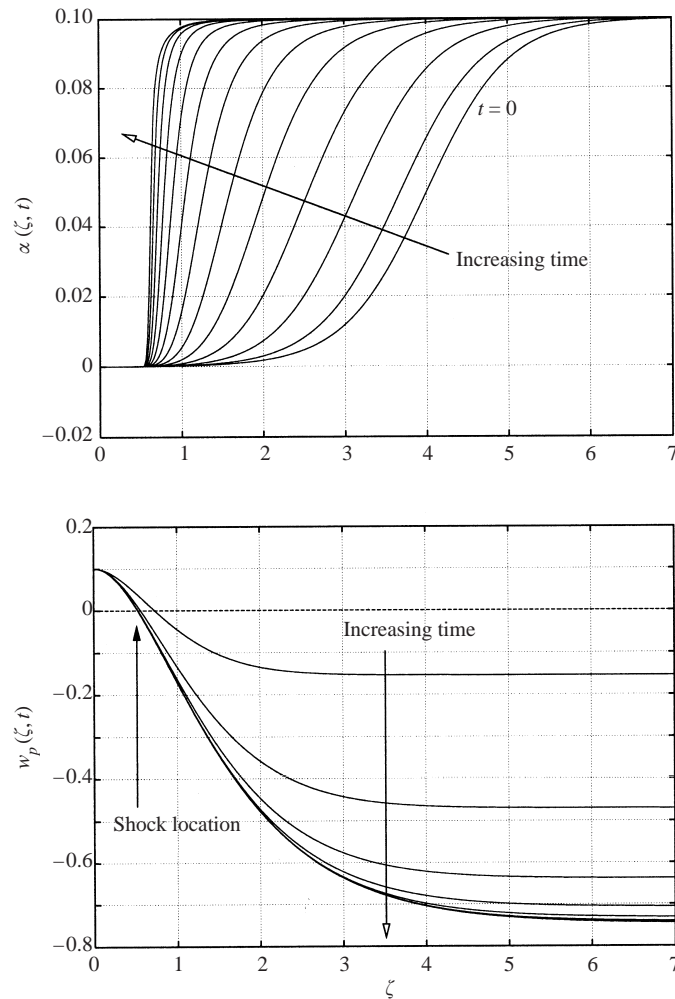


FIGURE 9. Evolution of the particle distribution function  $\alpha(\zeta, t)$  and axial particle velocity  $w_p(\zeta, t)$  for the case  $\mathcal{K} = -1$ ,  $\alpha_e \gamma = 0.1$ ,  $\beta/\gamma = 10$ . Note that in this case a shock develops in  $\alpha(\zeta, t)$  at a critical axial location where drag forces and the gravitational influence balance to give no axial particle velocity.

#### 4. Solution behaviour for large $\beta$

As noted above, the system (2.1)–(2.2b) is formally valid only in the limit of  $\beta \rightarrow \infty$  (corresponding to particle dimensions significantly smaller than the boundary-layer thickness); fortunately, in this limit some asymptotic progress is possible, and this is the focus of our attention in this section. This asymptotic work also serves to reinforce some of the conclusions gleaned from the previous section.

##### 4.1. Negligible gravity: $\mathcal{K} \approx 0$

For large  $\beta$ , we can write the solution for the velocity and particle concentration as an asymptotic series, although in this limit the description in some cases requires very thin wall layers. Clearly a requirement on our continuum formulation for dusty-gas flow is that any lengthscales ( $\Delta\zeta$ ) associated with the solution be large compared to



the particle size, which for the purposes of this section will require

$$\Delta\zeta \gg \beta^{-1/2}. \tag{4.1}$$

We shall find that for some of the asymptotic results presented below, (4.1) imposes more stringent conditions than have already been noted in (2.4); for now, all that we need to impose is

$$\beta \gg \gamma, \quad \beta \gg 1. \tag{4.2}$$

The asymptotic expansion for solutions of (2.10)–(2.16) for large  $\beta$  then proceeds as

$$\alpha = \frac{1}{\gamma}\hat{\alpha} + \dots, \tag{4.3}$$

$$\mathbf{u} = \mathbf{u}^{(0)} + \frac{\gamma}{\beta}\mathbf{u}^{(1)} + \dots, \quad \mathbf{u}_p = \mathbf{u}^{(0)} + \frac{\gamma}{\beta}\mathbf{u}_p^{(1)} + \dots, \quad \hat{\alpha} = \hat{\alpha}^{(0)} + \frac{\gamma}{\beta}\hat{\alpha}^{(1)} + \dots, \tag{4.4}$$

where, crucially, we note that to leading order the velocity of the fluid particles is equal to that of the fluid. This expansion and leading-order identity of the two velocity vectors has also been performed by UG. Substitution into (2.10)–(2.13) gives the equations

$$\dot{u}^{(0)} + w^{(0)}u^{(0)\prime} + u^{(0)2} - v^{(0)2} = u^{(0)\prime\prime} - \hat{\alpha}^{(0)}(u^{(1)} - u_p^{(1)}), \tag{4.5}$$

$$\dot{v}^{(0)} + w^{(0)}v^{(0)\prime} + 2u^{(0)}v^{(0)} = v^{(0)\prime\prime} - \hat{\alpha}^{(0)}(v^{(1)} - v_p^{(1)}), \tag{4.6}$$

$$\dot{u}^{(0)} + w^{(0)}u^{(0)\prime} + u^{(0)2} - v^{(0)2} = (u^{(1)} - u_p^{(1)}), \tag{4.7}$$

$$\dot{v}^{(0)} + w^{(0)}v^{(0)\prime} + 2u^{(0)}v^{(0)} = (v^{(1)} - v_p^{(1)}), \tag{4.8}$$

and (2.14)–(2.15) leads to the following equation for  $\hat{\alpha}^{(0)}$ :

$$\dot{\hat{\alpha}}^{(0)} + w^{(0)}\hat{\alpha}^{(0)\prime} = 0, \tag{4.9}$$

for which a solution consistent with the boundary values is simply  $\hat{\alpha}^{(0)} \equiv \hat{\alpha}_e$ . This being the case, (4.5)–(4.7) can be combined to form just two equations,

$$(\hat{\alpha}_e + 1)(\dot{u}^{(0)} + w^{(0)}u^{(0)\prime} + u^{(0)2} - v^{(0)2}) = u^{(0)\prime\prime}, \tag{4.10}$$

$$(\hat{\alpha}_e + 1)(\dot{v}^{(0)} + w^{(0)}v^{(0)\prime} + 2u^{(0)}v^{(0)}) = v^{(0)\prime\prime}. \tag{4.11}$$

These are the equations of the classical Kármán problem provided we make the simple transformations

$$\zeta = \left(\frac{1}{\hat{\alpha}_e + 1}\right)^{1/2} \hat{\zeta}, \quad w^{(0)} = \left(\frac{1}{\hat{\alpha}_e + 1}\right)^{1/2} \hat{w}^{(0)}. \tag{4.12}$$

Thus, we see that for non-dimensional times  $t \gg 1$ , the steady-state Kármán solution is established, although this leaves aside the question of what happens to the particle concentration,  $\hat{\alpha}$ , and whether or not the expansion (4.4) is valid for all  $\zeta$  and  $t$ . There is ample numerical evidence that the expansion is indeed uniformly valid in space and time for the horizontal velocity components,  $u$  and  $v$ . The development of the particle concentration is somewhat more interesting, and depends crucially on the presence or absence of significant gravitational force. It appears that modifications to the above results arise in some cases near the boundary, where (4.4) may fail. The nature of these near-wall structures seems to depend principally on the sign and the magnitude of  $\mathcal{H}$ .

4.1.1. Near-wall structures for  $\mathcal{K} \approx 0$ 

Returning to (2.15), substitution of the expansions for  $u$  and  $w$  leads to the following equation:

$$\hat{\alpha} + w^{(0)}\hat{\alpha}' + \frac{2\gamma}{\beta}\hat{\alpha} = 0. \quad (4.13)$$

Clearly, for large  $\beta$ , the conclusion is that to leading order in the expansion (4.3),  $\alpha$  is a constant, as we noted before. However, near the wall, continuity leads to  $w^{(0)} \sim -s\zeta^2$ , where  $s = -\frac{1}{2}w^{(0)'}|_{\zeta=0}$  (which may be calculated from the appropriate Kármán solution), and so for  $\zeta$  small, equation (4.13) becomes

$$\hat{\alpha}_t - s\zeta^2\hat{\alpha}_\zeta + \frac{2\gamma}{\beta}\hat{\alpha} = 0; \quad (4.14)$$

then the inner region implied by (4.14) can be rescaled by writing

$$\zeta = \left(\frac{2\gamma}{\beta s}\right)Z, \quad t = \frac{\beta}{2\gamma}\tau, \quad (4.15)$$

in which this inner equation for  $\alpha$  becomes

$$\hat{\alpha}_\tau - Z^2\hat{\alpha}_Z + \hat{\alpha} = 0. \quad (4.16)$$

The solution that satisfies the initial condition  $\alpha = \alpha_e$  and the boundary condition  $\alpha = \alpha_e$  at the edge of the layer is then

$$\hat{\alpha} = \begin{cases} \hat{\alpha}_e e^{-\tau}, & Z\tau < 1, \\ \hat{\alpha}_e e^{-1/Z}, & Z\tau > 1. \end{cases} \quad (4.17)$$

Therefore, for long times, there is a vanishingly small zone of width  $\tau^{-1}$  in  $Z$  in which  $\alpha$  continues to decay in time, and a zone that constitutes the majority of the wall layer in which  $\alpha$  is steady. Hence, for  $\beta \rightarrow \infty$ , there is no regular steady state at all, but rather an essential singularity develops, the solution for  $\alpha$  decreasing to zero more rapidly than any power or exponential of  $Z$ . The computations presented in §3 verify that the value of  $\alpha$  continues to change very slowly at the wall, as predicted here.

Before proceeding, we return briefly to the question of what restrictions need to be placed on the relative magnitudes of the parameters in the problem. As anticipated above, (4.1) leads to more severe limitations than either (2.4) or (4.2). In the analysis immediately above, we determined that there is a thin layer of width  $\gamma/\beta$  within the Kármán boundary layer. Consequently substitution into (4.1) gives a requirement that can be combined with (4.2) to give the restricted parameter range of the results,

$$\gamma^2 \gg \beta \gg \gamma \gg 1. \quad (4.18)$$

One might note an inconsistency here, since these are notionally heavy particles, and we have neglected gravitational effects. Though a gravitational influence will always exist for heavy particles, provided it only has an effect over a time that is long compared to the timescale under consideration, it can be ignored. This requirement is

$$\frac{g}{\sqrt{\nu}\Omega^3} \ll 1. \quad (4.19)$$

It is also important to note that (4.17) indicates that, as time increases, our continuum model for the particle distribution must ultimately fail, specifically when the thickness of this diminishing thin layer becomes comparable to the particle dimensions. As an aside, we note that it is because of the subtleties raised above that consistent numerical solutions of flows of this type have proved so difficult to obtain in the past.

4.2. Changes in the large- $\beta$  structure for  $\mathcal{K} \neq 0$

On including gravitational effects, depending on the relative ordering of  $\beta$  and  $\mathcal{K}$ , the expansion (4.4) may remain valid for large  $|\mathcal{K}|$ , but before addressing this issue, we turn to the vertical momentum equation for the particle phase, which will now be modified by the presence of the gravitational term,

$$\dot{w}^{(0)} + w^{(0)}w^{(0)\prime} = (w^{(1)} - w_p^{(1)}) - \mathcal{K}, \tag{4.20}$$

where we have retained the expansion (4.4). We discuss the question of appropriate wall conditions for arbitrary  $\beta$  in Appendix A, §A.2. Equation (4.20) appears to suggest that  $w_p^{(1)} = -\mathcal{K}$  at  $\zeta = 0$ ; however, this is incorrect for  $\mathcal{K} > 0$ , since the expansions (4.4) fail near the wall. Hence, we simply reiterate the results from Appendix A, §A.2 namely that for  $\mathcal{K} < 0$ ,  $w_p(\zeta = 0)$  can be arbitrarily specified (including setting  $w_p = 0$  at  $\zeta = 0$ ), whilst for  $\mathcal{K} > 0$ ,  $w_p(\zeta = 0)$  must be determined as part of the solution, although from our  $\beta \gg 1$  analysis, (A 16) tells us that

$$w_p = -\frac{\gamma\mathcal{K}}{\beta} \quad \text{on} \quad \zeta = 0. \tag{4.21}$$

This conclusion can be readily understood in both physical and mathematical terms. Physically, for a gravitational field directed towards the boundary ( $\mathcal{K} > 0$ ), particles sediment out of solution and ‘collide’ with the wall. Particles that descend from sufficiently large distances (i.e. many particle diameters) from the wall, will hit the wall at a ‘terminal velocity’, so that  $w_p$  clearly cannot be arbitrarily imposed. In line with our comments in the previous section, mathematically, for  $\mathcal{K} > 0$  (and hence  $w_p < 0$ ), all characteristics leaving  $t = 0$  in the  $(\zeta, t)$ -plane intersect  $\zeta = 0$  at a finite time; that is to say,  $(-\zeta, t)$  is a time-like direction.

Nevertheless, the behaviour of the solution to (2.16) is not immediately obvious for  $\mathcal{K} = O(1)$ , and so we turn now to a simpler case—that for very large  $|\mathcal{K}|$ , which (as we have noted) can be appropriate to a laboratory setting.

4.3. Large- $|\mathcal{K}|$  solutions

If the influence of gravity is sufficiently large, be it negative or positive (i.e. directed away from or towards the boundary), then in the vertical momentum equation, (2.16), the coupling term  $\beta w/\gamma$  can be neglected to first order. (Here we continue to assume that  $\beta$  is large, but not ‘too’ large compared with  $\mathcal{K}$ ; this requirement will be quantified shortly). In this case, (2.16) becomes

$$\dot{w}_p + w_p w_p' + \frac{\beta}{\gamma} w_p = -\mathcal{K}. \tag{4.22}$$

This equation can be solved exactly by the method of characteristics. Along a characteristic,

$$w_p = -\frac{\gamma\mathcal{K}}{\beta} + C_1 e^{-\beta t/\gamma} \tag{4.23}$$

on

$$\zeta + C_2 = -\frac{\gamma\mathcal{K}}{\beta} t - \frac{\gamma C_1}{\beta} e^{-\beta t/\gamma}. \tag{4.24}$$

The constants  $C_1$  and  $C_2$  are determined by application of particular boundary and/or initial conditions. Below, we explore the two sub-cases,  $\mathcal{K} \ll -1$  and  $\mathcal{K} \gg 1$ .

4.3.1.  $\mathcal{K} \ll -1$ : Gravity acting away from the boundary

The  $(w_p, \alpha)$  solutions

Suppose that the initial and boundary conditions are as given in §2.3, namely

$$w_p = -\frac{\gamma\mathcal{K}}{\beta} \quad \text{at } t = 0 \text{ for all } \zeta; \quad w_p = 0 \quad \text{at } \zeta = 0 \text{ for all } t. \quad (4.25)$$

The characteristic map from (4.23) and (4.24) indicates that there is an expansion wave emanating from  $\zeta = t = 0$  in the  $(\zeta, t)$  plane). Let that wave occupy the region in the plane between  $\zeta_{d+}(t)$  and  $\zeta_{d-}(t)$ . For  $\zeta > \zeta_{d+}$ ,  $C_1$  in (4.23) is taken to be zero to satisfy the initial condition in (4.25). In that case, (4.24) shows the characteristics in that zone to be given by  $\zeta + \gamma\mathcal{K}t/\beta = \text{const}$ . The boundary of this zone is then given by  $\zeta_{d+} = -\gamma\mathcal{K}t/\beta$ . Thus, we have

$$w_p = -\frac{\gamma\mathcal{K}}{\beta} \quad \text{for } \zeta > \zeta_{d+} = -\frac{\gamma\mathcal{K}}{\beta}t. \quad (4.26)$$

In the region determined by the boundary condition in (4.25),  $\zeta < \zeta_{d-}$ , and in this region, (4.23) and (4.25) indicate that  $C_1 = (\gamma\mathcal{K}/\beta)\exp(\beta t_o/\gamma)$ , where  $t_o \geq 0$  on  $\zeta = 0$ . From (4.24), the characteristics in this region are given by

$$\zeta + \frac{\gamma\mathcal{K}}{\beta}t + \frac{\gamma^2\mathcal{K}}{\beta^2}(e^{\beta(t_o-t)/\gamma} - 1) = \frac{\gamma\mathcal{K}}{\beta}t_o. \quad (4.27)$$

Setting  $t_o = 0$  gives the delimiter of this region,

$$\zeta_{d-} = -\frac{\gamma\mathcal{K}}{\beta}t - \frac{\gamma^2\mathcal{K}}{\beta^2}(e^{-\beta t/\gamma} - 1). \quad (4.28)$$

Then, eliminating  $t_o$  between  $C_1$  and (4.27) gives  $w_p$  implicitly in this region as

$$\zeta = \frac{\gamma^2\mathcal{K}}{\beta^2} \log \left( 1 + \frac{\beta w_p}{\gamma\mathcal{K}} \right) - \frac{\gamma}{\beta} w_p \quad \text{for } \zeta < \zeta_{d-}. \quad (4.29)$$

Note that this solution is time-independent.

In the zone  $\zeta_{d-} < \zeta < \zeta_{d+}$ , all characteristics must pass through  $\zeta = t = 0$ , so by (4.24),

$$C_1 = \frac{\beta\zeta + (\gamma\mathcal{K}/\beta)t}{\gamma e^{-\beta t/\gamma} - 1}.$$

Substitution of this  $C_1$  into (4.23) gives  $w_p$  in the expansion wave,

$$w_p = -\frac{\gamma\mathcal{K}}{\beta} + \frac{\beta\zeta + (\gamma\mathcal{K}/\beta)t}{\gamma e^{\beta t/\gamma} - 1} \quad \text{for } \zeta_{d-} < \zeta < \zeta_{d+}. \quad (4.30)$$

Figure 10 shows this solution versus  $\zeta$  for a particular time  $t$ . Two features should be noted: (i)  $w_p$  is continuous, but with discontinuous derivatives; (ii) for  $t \gg \gamma/\beta$ ,  $w_p \rightarrow -\gamma\mathcal{K}/\beta$  in  $\zeta < \zeta_{d-}$ , since  $\zeta_{d+}$  and  $\zeta_{d-}$  are indistinguishable for such long times.

Examination of the equation for the particle concentration,  $\alpha$ , in this layer, under the large- $|\mathcal{K}|$  assumption, gives the approximate version of (2.15) as

$$\dot{\alpha} + w_p\alpha' + w_p'\alpha = 0. \quad (4.31)$$

Careful construction of the characteristic solution to this equation indicates that  $\alpha$  in

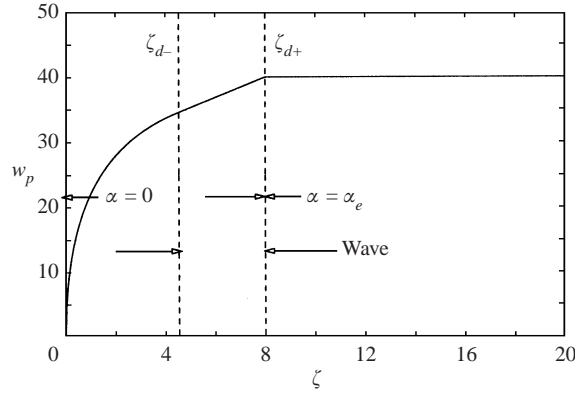


FIGURE 10. The asymptotic vertical particle velocity and volume fraction profiles for  $\mathcal{K} = -400, \beta = 20, \gamma = 2$  at  $t = 0.2$ ; as determined from (4.30).

this solution is discontinuous, and given by

$$\alpha = \begin{cases} 0, & \zeta < \zeta_{d+}, \\ \alpha_e, & \zeta > \zeta_{d+}. \end{cases} \quad (4.32)$$

From (4.28), for example, the layer width scales as  $\gamma^2 \mathcal{K} / \beta^2$ , and so according to (4.1) the quantity  $\mathcal{K}$  must be large enough to satisfy the requirement

$$|\mathcal{K}| \gamma^2 \gg \beta^{3/2}. \quad (4.33)$$

(The neglect of the  $w$  term in (4.22) gives a weaker restriction,  $\gamma |\mathcal{K}| \gg \beta$ .) This solution can be constructed for any value of  $w_p$  at  $\zeta = 0$  and  $t = 0$ , with no qualitative alteration in the results. The significant point is that the characteristics have positive slope, so information is carried out, away from both  $\zeta = 0$  and  $t = 0$ . It is also important to note that the layer continues to grow and hence there is no steady-state solution: the wave between  $\zeta_{d+}$  and  $\zeta_{d-}$  grows for all time. Though this result is clearly valid regardless of the size of  $\beta$ , if  $\beta$  also large, as we have assumed above, then the  $w_p$  term in (2.16) is always larger than the ‘ $w$ ’ term, so that its neglect is justified.

The solutions given for  $w_p$  and  $\alpha$  evaluated above are independent, under (4.33), of the horizontal components. The structure of the horizontal motion does, however, depend on  $(w_p, \alpha)$ , as we shall see below.

#### The horizontal velocity components

As the front illustrated in figure 11 propagates outward through the layer, the horizontal velocity components are also varying in time in the two regions. Beneath the front at  $\zeta_d$ , since  $\alpha \equiv 0$ , the standard no-particle equations of motion are valid. Beyond the front, where  $\alpha = \alpha_e$ , the full equations are required. Solutions in the two regions are joined at  $\zeta_d$ . The horizontal velocities evolve on an  $O(1)$  timescale, but when  $t = O(1)$ , the front is already at the edge of the boundary layer or beyond, according to figure 11. However, near the edge of the layer,  $u, v, u_p$  and  $v_p$  are all exponentially small. Therefore, the remainder of the transient adjustment in the layer occurs in a fashion that is identical to a case with no particles. (Obviously, for  $\zeta < \zeta_d$

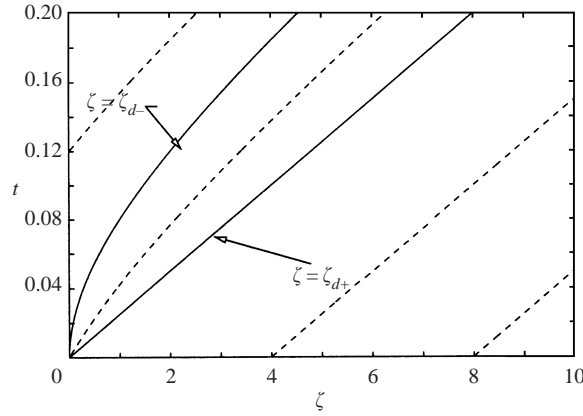


FIGURE 11. The characteristic map for  $\mathcal{K} \ll -1$  showing the expansion wave emanating from the origin.

values for  $u_p$  and  $v_p$  may be found directly from

$$\begin{aligned} \dot{u}_p + w_p u'_p + u_p^2 - v_p^2 + \frac{\beta}{\gamma} u_p &= \frac{\beta}{\gamma} u(\zeta, t), \\ \dot{v}_p + w_p v'_p + 2u_p v_p + \frac{\beta}{\gamma} v_p &= \frac{\beta}{\gamma} v(\zeta, t), \end{aligned} \quad (4.34)$$

by inserting the  $(u, v)$  from the no-particle Kármán problem, but there is no real point in writing down solutions, since there are no particles in that zone anyway.)

#### 4.3.2. $\mathcal{K} \gg 1$ : Gravity acting towards the boundary

In this heavy-particle case, the characteristic directions have negative slope in the  $(\zeta, t)$ -plane, so all characteristics beginning on  $t = 0$  intersect  $\zeta = 0$ , with  $w_p$  varying along each according to (4.23). Hence, we have

$$w_p = -\frac{\gamma \mathcal{K}}{\beta} \quad \text{for all } \zeta, t. \quad (4.35)$$

Note that if the initial condition, instead of a uniform gravitationally induced vertical motion, is  $w_p = 0$ , then the vertical velocity is time-dependent, and given by

$$w_p = \frac{\gamma \mathcal{K}}{\beta} [e^{-\beta t/\gamma} - 1] \quad \text{for all } \zeta, t. \quad (4.36)$$

Then, equation (4.31) can also be easily solved, with the conclusion that

$$\alpha = \alpha_e. \quad (4.37)$$

This is consistent with (4.10) and (4.10), therefore we have found that at large and positive  $\mathcal{K}$ , the problem does indeed have a steady state, essentially like the no-particle problem, with a uniform particle distribution across the layer, provided that (4.33) is satisfied once again.

We also note that if instead there is an initial distribution for  $\alpha$  given by, say,  $\alpha_i(\zeta)$ , then the solution for that case at later times is

$$\alpha = \alpha_i \left( \zeta + \frac{\mathcal{K} \gamma t}{\beta} + \frac{\gamma^2 \mathcal{K}}{\beta^2} [e^{-\beta t/\gamma} - 1] \right). \quad (4.38)$$

Unlike the situation in §4.3.1 above, if  $\beta$  is large, then (4.33) implies that  $(u_p, v_p) \ll (u, v)$ . Though the unsteady development is rather complicated, the steady state has the leading-order form (where all quantities are functions of a scaled variable,  $\bar{\zeta} = \beta^{1/2}\zeta$ ),

$$u = -\frac{1}{3\alpha_e\beta} [\exp(-2\sqrt{\alpha_e\bar{\zeta}}) - \exp(-\sqrt{\alpha_e\bar{\zeta}})] + \dots, \quad v = \exp(-\sqrt{\alpha_e\bar{\zeta}}) + \dots, \quad (4.39a)$$

$$u_p = \frac{\beta^{1/2}}{6\alpha_e^{3/2}\gamma^2\mathcal{K}} [2\exp(-\sqrt{\alpha_e\bar{\zeta}}) - \exp(-2\sqrt{\alpha_e\bar{\zeta}})] + \dots,$$

$$v_p = \frac{\beta^{3/2}}{\alpha_e^{1/2}\gamma^2\mathcal{K}} \exp(-\sqrt{\alpha_e\bar{\zeta}}) + \dots, \quad (4.39b)$$

$$w = \frac{1}{3\alpha_e^{3/2}\beta^{3/2}} [2\exp(-\sqrt{\alpha_e\bar{\zeta}}) - \exp(-2\sqrt{\alpha_e\bar{\zeta}}) - 1] + \dots, \quad (4.39c)$$

$$w_p = -\frac{\mathcal{K}\gamma}{\beta} - \frac{1}{3\alpha_e^2\beta^{3/2}} + \frac{1}{6\alpha_e^2\gamma^2\mathcal{K}} [\exp(-2\sqrt{\alpha_e\bar{\zeta}}) - 4\exp(-\sqrt{\alpha_e\bar{\zeta}})] + \dots, \quad (4.39d)$$

$$\alpha = \alpha_e - \frac{\beta}{3\alpha_e\gamma^3\mathcal{K}^2} [4\exp(-\sqrt{\alpha_e\bar{\zeta}}) - \exp(-2\sqrt{\alpha_e\bar{\zeta}})] + \dots. \quad (4.39e)$$

Consequently, as in the  $\mathcal{K} = 0$  case, the particle slip velocity components are deduced as a part of the solution. Note too that the particle concentration at the surface is somewhat less than  $\alpha_e$ , consistent with the trend found numerically, which is shown in figure 7. It should be pointed out that the constant value of  $w_{p1}$  is determined in order to render the  $w_p$  series uniformly valid in  $\zeta$ , that is, by making  $w_{p1} = w_0(\infty)$ .

Other asymptotic values are possible, but less important. In Appendix B, however, we give details of the small-time development of the solution (for order-one parameter values), and this is in agreement with a number of key features described above.

## 5. Conclusions

We have considered the problem of spin-up of a fluid with a dilute suspension of small particles both with and without the effects of gravity. Although we formally only consider particles whose density relative to the fluid is large, the associated influence of gravity can act either in the same direction as or in the opposite direction to the Ekman axial flow induced by the rotation of the boundary. In terms of an experimental configuration, these two cases correspond to the fluid being above or below the rotating plane respectively, with gravity acting vertically.

The system of equations at the heart of our study may be considered somewhat heuristic for order-one parameter values. Nevertheless, in the various parameter regimes that have been the main focus of our attention (in particular (i) small particle concentrations, (ii) particle size  $\ll$  boundary-layer thickness, (iii) particle density  $\gg$  fluid density), we believe our model becomes formally correct. Mathematically the system employed can model a rich blend of parabolic- and hyperbolic-type behaviours.

The problem has revealed a number of important subtleties, which go some way in explaining the difficulties encountered in previous studies. Not the least of these is the development (in the zero-gravity, large- $\beta$  case) of an essential singularity in the particle concentration distribution close to the wall (as described by equation (4.17)). We can therefore observe that no steady, regular state exists to the problem, but rather there is a zone in the immediate vicinity of the disk which continues to

diminish in thickness as time increases (although ultimately those restrictions in our model, in particular the smallness of the particles compared with all boundary-layer scales, must be violated by this large-time behaviour).

The influence of gravity (which has not been directly addressed in the past in this class of problem, as far as we are aware) has a profound influence on the solution structure. The direction of the gravitational field, relative to the particle drag resulting from the axial Ekman suction, is crucial here. When the gravitational acceleration is directed towards the rotating boundary, particles are drawn in from the outer extremes of the boundary layer, by both the Ekman suction and gravity, and will ultimately collide with the bounding plane. Under these circumstances, our model does not permit the enforcement of any particle boundary conditions on the disk (but rather demands far-field boundary conditions). A more complete model involving particle/wall interactions would have to take these effects into account, presumably through the presence of a sublayer of sorts, utilizing the particle conditions as calculated from the model proposed here; again, we do not regard this as a central issue for the current paper. In this respect, experimental information of the particle-wall mechanics will clearly prove useful.

When the local gravitational acceleration is directed away from the rotating boundary, close to the wall, particles will be transported away, leading ultimately to a particle-free zone, which may (as time increases) lead to a discontinuity in the particle distribution function at some finite distance from the disk surface. This location may be regarded as that point at which the drag forces associated with the Ekman suction precisely balance with the gravity force acting on the particles; this is effectively an equilibrium point in terms of the axial motion of the particle phase. The formation of such a point, and indeed the development of an associated discontinuity in particle distribution, is clearly seen in figure 9, and is discussed analytically for the short-time behaviour in Appendix B. In this regime, it is mathematically consistent to impose conditions on the behaviour of the particle phase at the wall, although as noted in the text there is no physical interpretation of the particle velocities, if there are no particles in this vicinity!

However, under these circumstances the imposition of particle velocity boundary conditions at the wall seems to play absolutely no role in determining particle velocities in regions where particles are actually present. This irrelevance of the surface  $(u_p, v_p)$  components is clearly shown in Appendix B, where we indicate that eigenfunctions arise in the layer near the wall, whose amplitude depends on the wall boundary conditions, but which vanish at the front *per se*. Furthermore this point can be confirmed numerically, as illustrated by figure 12. In our opinion, this (physically) meaningful result adds yet further credence to this choice of model equations. Again, a full analysis that also directly models the issue of particle distribution behaviour at the wall would be useful, but is not central to the theme of this work; our emphasis here is deliberately focused on the core fluid mechanics arising from problems of this class.

The recent interesting paper by Slater & Young (2001) was brought to the attention of the authors by a referee. This work treats problems in which the particle phase is decoupled from the continuous-phase equation. One of the issues discussed is that of 'shadow zones' (in which the particle concentration is zero) which the numerical method treats through a 'virtual' particle distribution that satisfies prescribed conditions at the solid boundaries. There is clearly some theoretical support for such an approach in the more mathematical description here, where it is seen that the prescribed wall conditions in fact have little influence except in the shadow zone for a whole range of boundary conditions.



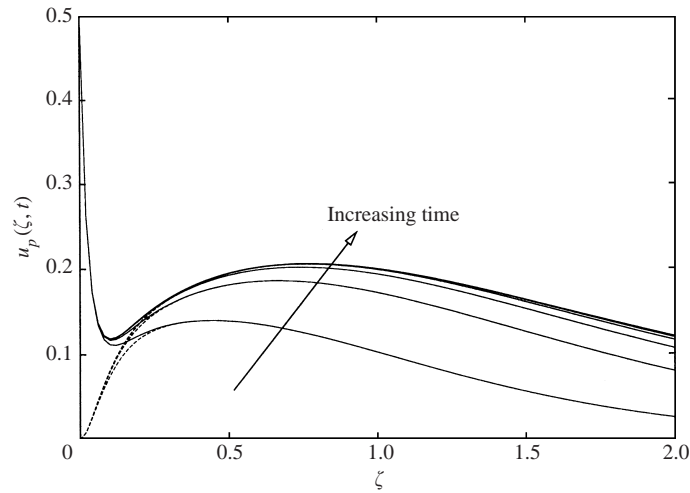


FIGURE 12. The near-wall evolution of  $u_p(\zeta, t)$  for  $\mathcal{K} = -5$ ,  $\alpha_e \gamma = 0.1$ ,  $\beta/\gamma = 10$  (this figure only shows a sub-region of a much larger computational domain). The evolutions are shown with two different wall boundary conditions:  $u_p(\zeta = 0, t) = 0$  (dashed lines) and  $u_p(\zeta = 0, t) = 0.5$  (solid lines). The difference between the two is contained in a near-wall region as suggested by the analysis of Appendix C. In this case, the axial particle velocity,  $w_p(\zeta, t)$ , develops a zero at  $\zeta \approx 1.72$ .

Finally, Li & Ahmadi (1993) have given a useful generalization of the Saffman force in a multi-dimensional flow, showing that it scales with

$$\rho_f a^2 (\nu D)^{1/2} \Omega r,$$

where  $D$  is the scale of the deformation tensor in the flow. A referee has pointed out, as is also noted in Osipov (1997), that such a force can be very important in boundary-layer regions. Taking the ratio of this force to the Stokes drag gives

$$\frac{\text{Saffman force}}{\text{Stokes drag}} = O\left(\frac{r/a}{\beta^{3/2}}\right).$$

Since this expression is the ratio of two large quantities, the Saffman force can indeed be important. We postpone for future investigation the incorporation of the Saffman force into the problem studied, although certainly for  $\beta$  sufficiently large, it can be neglected.

We hope that this work will provide impetus for experimental comparisons to be undertaken in the near future. The analysis and computations have indicated a number of significant physical processes and phenomena that may be expected to occur in a complex three-dimensional flow, and will provide a stringent test that is amenable to experimental comparisons whilst also indicating which parameter regimes should be examined in the laboratory. Equally, if the validity of our governing equations can be confirmed for the present problem, then these equations (in particular those relating to the particle phase) should be equally applicable to many other flows involving dilute particle suspensions.

The authors wish to express their gratitude to Professor Peter Davies for a number of useful discussions connected with the physical aspects of the problem. The support of the EPSRC is gratefully acknowledged. Three referees have also made suggestions that have significantly strengthened this paper.

## Appendix A. Time evolution of surface conditions

### A.1. Flow with negligible gravity: $\mathcal{K} \approx 0$

Interestingly, since there are no diffusion terms in the particle-velocity equations, these can be evaluated at the disk surface and their temporal evolution determined independently of any behaviour elsewhere in the boundary layer.

Evaluating equations (2.12) and (2.13) at the surface, under the assumption of impermeability (2.20), which as we shall see is sensible for  $\mathcal{K} \approx 0$ , gives

$$\dot{u}_{po} + u_{po}^2 - v_{po}^2 + \frac{\beta}{\gamma} u_{po} = 0, \quad (\text{A } 1)$$

$$\dot{v}_{po} + 2u_{po}v_{po} + \frac{\beta}{\gamma}(v_{po} - 1) = 0. \quad (\text{A } 2)$$

We come later to the situation at the surface for  $\mathcal{K} \neq 0$ . The subscript ‘ $po$ ’ indicates a particle speed evaluated at the surface,  $\zeta = 0$ . Note that these equations are decoupled from the vertical momentum and particle concentration equations.

The particle continuity equation, (2.15), similarly takes the form

$$\dot{\alpha}_o + \alpha_o(2u_{po} + A) = 0, \quad (\text{A } 3)$$

where, for brevity, we have written  $A = w'_p(\zeta = 0)$ . Finally, (2.16) is an identity evaluated at the surface, provided  $\mathcal{K}$  is sufficiently small. Differentiating this equation with respect to  $\zeta$ , we obtain

$$\dot{w}'_p + (w'_p)^2 + w_p w''_p = \frac{\beta}{\gamma}(w' - w'_p). \quad (\text{A } 4)$$

Note from (2.14) that because of no slip,  $w' \equiv 0$  at the surface. Hence, (A 4) evaluated at  $\zeta = 0$  becomes an evolution equation for  $A$ ,

$$\dot{A} + A^2 + \frac{\beta}{\gamma}A = 0. \quad (\text{A } 5)$$

The solution is easily found:

$$A = \frac{A(0)}{[1 + (\gamma/\beta)A(0)] \exp(\beta t/\gamma) - (\gamma/\beta)A(0)}, \quad (\text{A } 6)$$

and so clearly a singularity may develop in a finite time if and only if

$$\frac{\gamma}{\beta}A(0) < -1; \quad (\text{A } 7)$$

the time for singularity formation is then

$$t_s = -\frac{\gamma}{\beta} \log \left( 1 + \frac{\beta}{\gamma A(0)} \right). \quad (\text{A } 8)$$

However, in the specific configurations to be studied here (which are also likely to be the most realizable, experimentally)  $A(0) = 0$ , and so  $A \equiv 0$  for all time. The aforementioned finite-time singularities, the question of their realization through an initial-value process and their physical interpretation are subjects for future investigation.

A.1.1. Long-time behaviour

Equations (A 1), (A 2) have fixed points, given by solution of the equations

$$u_{po}^2 - v_{po}^2 + \frac{\beta}{\gamma}u_{po} = 0, \quad 2u_{po}v_{po} + \frac{\beta}{\gamma}(v_{po} - 1) = 0. \tag{A 9}$$

Combining gives the quartic equation

$$u_{po} \left( u_{po} + \frac{\beta}{\gamma} \right) \left( 1 + \frac{2\gamma}{\beta}u_{po} \right)^2 = 1, \tag{A 10}$$

and then

$$v_{po} = \frac{1}{1 + (2\gamma/\beta)u_{po}}. \tag{A 11}$$

The quartic (A 10) has two real solutions: one positive and one negative. Phase-plane analysis of the equation pair (A 1), (A 2) shows that the positive root is a stable fixed point, and the negative root is an unstable fixed point, so all initial conditions lead eventually to the  $u_{po} > 0$  root.

Since we know that  $A \rightarrow 0$  for long time (assuming the absence of any finite-time singularities), the corresponding behaviour of  $\alpha_o$ , from (A 3), is given by solution of

$$\dot{\alpha}_o + 2u_{po}\alpha_o = 0, \tag{A 12}$$

and so

$$\alpha_o \sim Ce^{-2u_{po}t} \quad \text{as } t \rightarrow \infty. \tag{A 13}$$

A.2. Surface conditions for  $\mathcal{K} \neq 0$

The situation with respect to surface conditions is fundamentally different for  $\mathcal{K} < 0$  and  $\mathcal{K} > 0$ . Inspection of (2.16) indicates that  $w_p \neq 0$  at  $\zeta = 0$  for  $\mathcal{K} \neq 0$ . In fact, a more careful examination suggests the following possible small- $\zeta$  behaviour if  $w_p(\zeta = 0)$  is set to zero:

$$w_p = \sqrt{-2\mathcal{K}\zeta} - \frac{2\beta}{3\gamma}\zeta + \dots \tag{A 14}$$

Obviously, for  $\mathcal{K} = 0$ , the first term is absent, and therefore (A 14) is consistent with the description provided in the preceding section.

For  $\mathcal{K} < 0$ ,  $w_p$  may be zero at the surface. We shall see in subsequent sections, however, that it is possible to specify  $w_p$  (arbitrarily) at  $\zeta = 0$  for  $\mathcal{K} < 0$ , in which case the expansion

$$w_p = A_0(t) + \zeta A_1(t) + \dots, \quad \mathcal{K} < 0, \tag{A 15}$$

is the proper one, and substitution of this into (2.16) gives

$$\dot{A}_0 + \frac{\beta}{\gamma}A_0 + A_0A_1 = -\mathcal{K}. \tag{A 16}$$

Therefore, with  $A_0$  specified,  $A_1$  can be determined.

If  $\mathcal{K} > 0$ , then clearly (A 14) fails, suggesting that in such a case  $A_0$  must be non-zero so that (A 16) is appropriate for calculating  $A_1$ . Thus we conclude that, for  $\mathcal{K} < 0$ ,  $w_p$  may be zero at the surface, or take a prescribed non-zero value; however, for  $\mathcal{K} > 0$ ,  $w_p$  must be non-zero at the surface. In fact, the value of  $w_p$  at  $\zeta = 0$  in this latter case cannot be specified arbitrarily, but rather is determined by conditions off the wall.

**Appendix B. Short-time behaviour of the solution**

It is helpful to examine the behaviour of the solutions for short times as this provides some further guidance for the development of appropriate numerical techniques, and gives still further insight into the physics. Here we again assume that the initial state is that of uniform particle settling/rising ( $w_p = -\gamma\mathcal{K}/\beta$ ), and uniform volume ratio ( $\alpha = \alpha_e$ ), with no initial fluid motion.

**B.1.  $\mathcal{K} \approx 0$**

In the absence of a significant gravitational body force, the system (2.10)–(2.16) possesses a small-time expansion of the form

$$u = u_0(\eta)t + \dots, \quad v = v_0(\eta) + \dots, \quad w = w_0(\eta)t^{3/2} + \dots, \tag{B 1a}$$

$$u_p = u_{p0}(\eta)t^2 + \dots, \quad v_p = v_{p0}(\eta)t + \dots, \quad w_p = w_{p0}(\eta)t^{5/2} + \dots. \tag{B 1b}$$

Here,  $\eta = O(1)$  represents the usual scaled coordinate  $\zeta = \eta t^{1/2}$ , and  $\alpha = \alpha_e + \dots$ , where  $\alpha_e$  is the initial particle concentration, which in line with our assumed initial conditions must be uniform.

The leading-order equations for the fluid phase are unchanged from those found as  $t \rightarrow 0$  in the single-phase Kármán problem, namely

$$u_0 - \frac{\eta}{2}u_0' - v_0^2 = u_0'', \quad -\frac{\eta}{2}v_0' = v_0'', \quad 2u_0 + w_0' = 0. \tag{B 2a-c}$$

The solution for the particle phase is easily determined subsequent to evaluation of  $u_0, v_0$  and  $w_0$ , yielding

$$u_{p0}(\eta) = -\frac{2\beta\eta^4}{\gamma} \int_{\infty}^{\eta} \frac{u_0(s)}{s^5} ds, \tag{B 3a}$$

$$v_{p0}(\eta) = -\frac{2\beta\eta^2}{\gamma} \int_{\infty}^{\eta} \frac{v_0(s)}{s^3} ds, \tag{B 3b}$$

$$w_{p0}(\eta) = -\frac{2\beta\eta^5}{\gamma} \int_{\infty}^{\eta} \frac{w_0(s)}{s^6} ds. \tag{B 3c}$$

There is a slight additional complication in the small-time behaviour of the two-phase problem; since the fluid phase satisfies no-slip conditions at the disk, this drives an azimuthal particle motion that is important to leading order in (2.12). This results in a passive inner region defined by  $\zeta = \xi t^{3/2}$ , within which a balance between  $\dot{u}_p$  and  $v_p^2$  can be achieved. For completeness, we note that in this inner layer adjacent to the disk, the particle-phase velocity components are

$$u = \bar{u}_{p0}(\xi)t^3 + \dots, \quad v = \bar{v}_{p0}(\xi)t + \dots, \quad w = \bar{w}_{p0}(\xi)t^{9/2} + \dots. \tag{B 4}$$

**B.2.  $\mathcal{K} < 0$**

For  $\mathcal{K} < 0$ , the boundary layer again has a double structure at short times, and expansions (B 1a), (B 1b) remain correct for the horizontal components, except very near the wall. However in (B 1b) the expansion for the vertical component,  $w_p$ , must be replaced by

$$w_p = -\frac{\gamma\mathcal{K}}{\beta} + w_{p0}(\eta) t^{5/2} + \dots, \tag{B 5}$$

although  $w_{p0}$  is still given by (B 3c).

For the near-wall particle-velocity components described below, it is important to note that the analysis of the  $w_p$  equation in §4.3.1 for large  $\beta$  and  $\mathcal{K}$  is valid here,

since at short times, the  $w$  term in the  $w_p$  equation is of higher order, just as in that case, but for different reasons. Here, neglect of this term requires that

$$t \ll \left(-\frac{\gamma \mathcal{K}}{\beta}\right)^{2/3}. \tag{B 6}$$

From (4.26)–(4.30), the vertical velocity at short times is given by these large- $|\mathcal{K}|$  results. Hence,

$$w_p = \begin{cases} (-2\mathcal{K}\zeta)^{1/2}, & \zeta < \zeta_{d-}, \\ \zeta/t - \frac{1}{2}\mathcal{K}t, & \zeta_{d-} < \zeta < \zeta_{d+}, \\ -\gamma\mathcal{K}/\beta, & \zeta > \zeta_{d+}. \end{cases} \tag{B 7}$$

The leading and trailing edges of the expansion wave are given for short times by

$$\zeta_{d+} = -\frac{\gamma\mathcal{K}t}{\beta}, \quad \zeta_{d-} \approx -\frac{1}{2}\mathcal{K}t^2. \tag{B 8}$$

Note that this result is consistent with that of (B 5). The results (B 8) follow from approximating (4.28) and (4.26) for short times. Substitution of this form for  $w_p$  and the horizontal fluid component expansion into the equations for the horizontal particle-velocity components indicates that the expansions (B 1*b*) fail for  $\zeta = O(t)$ . An asymptotic expansion in this near-wall region is

$$u_p \sim \frac{2\beta}{3\gamma}u'_0(0) \left[\frac{\zeta}{t} + \frac{2}{5}\left(\frac{\gamma\mathcal{K}}{\beta} - \frac{\beta}{\gamma}\zeta\right)\right] t^{5/2} + O(t^{7/2}, \zeta^2), \tag{B 9}$$

$$v_p \sim \frac{\beta}{\gamma}[t + 2v'_0(0)t^{1/2}\zeta] + O(t^2, \zeta^2) \quad \text{for } \zeta > \zeta_{d+}. \tag{B 10}$$

This solution in this region, valid for  $\zeta = O(t)$ , is a series of terms in the form  $\zeta^m t^n$ . Notice that taking  $\zeta \rightarrow \infty$  in this expansion, then rewriting in terms of  $\eta$ , confirms the matching with the base of the  $\eta$  layer, where the solutions are given by (B 1*b*).

At the upper edge of the expansion wave, the particle-velocity components take the form

$$\left. \begin{aligned} u_p &= -\frac{2}{5}\mathcal{K}u'_0(0)t^{5/2} + O(t^3), \\ v_p &= \frac{\beta}{\gamma}t + O(t^{3/2}) \quad \text{at } \zeta = \zeta_{d+}. \end{aligned} \right\} \tag{B 11}$$

The solutions (B 9) and (B 10) are above the leading-edge of the front; again,  $u_p$  and  $v_p$  are physically meaningless for  $\zeta < \zeta_{d+}$ , where  $\alpha \equiv 0$ . On the other hand, in the numerical solutions, we must compute both  $u_p$  and  $v_p$  in the region  $\zeta < \zeta_{d+}$ . With a view to exploring that issue, we insert result (B 7) for  $\zeta < \zeta_{d-}$  into the equations for  $u_p$  and  $v_p$ , and the solutions below the trailing edge of the wave are

$$\left. \begin{aligned} u_p &\sim -\frac{\beta\mathcal{K}}{3\gamma}u'_0(0) \left[\phi - \frac{4}{5}\sqrt{\phi} + \frac{8}{35}\right] t^{7/2} + A_1(\sqrt{\phi} - 1)^{7/2}t^{7/2}, \\ v_p &\sim \frac{\beta}{\gamma}t + A_2(\sqrt{\phi} - 1) \quad \text{for } \zeta < \zeta_{d-}, \end{aligned} \right\} \tag{B 12}$$

where  $\phi \equiv -2\zeta/\mathcal{K}t^2$ , so that  $\phi = 1$  at  $\zeta = \zeta_{d-}$ . The quantities  $A_1$  and  $A_2$  are arbitrary constants, and are clearly determined by whatever boundary conditions are given for  $u_p$  and  $v_p$  at the wall. Nevertheless, these eigenfunctions vanish at  $\phi = 1$ . The importance of this result is that any choice for wall values for  $u_p$  and  $v_p$  has no

effect on the solution where the particle velocities have meaning, that is, in the region  $\zeta > \zeta_d$ . Similar solutions can be constructed in  $\zeta_{d-} < \zeta < \zeta_{d+}$ , and that process gives

$$\left. \begin{aligned} u_p &\sim -\frac{\beta \mathcal{K}}{\gamma} u'_0(0) \left[ \frac{1}{7} + \frac{\phi - 1}{5} \right], \\ v_p &\sim \frac{\beta}{\gamma} t \quad \text{for } \zeta_{d-} < \zeta < \zeta_{d+}. \end{aligned} \right\} \quad (\text{B } 13)$$

This solution connects to (B 12) at  $\phi = 1$  below, and to (B 11) for  $\phi \sim 2\gamma/(\beta t)$ . Eigenfunctions also arise in this region, but must be zero in order for the solution to connect to (B 11).

As we have noted throughout the paper, in the case  $\mathcal{K} < 0$  the characteristics are directed away from the plane at  $\zeta = 0$  and one is at liberty to specify the boundary conditions at this point for the particle phase. However, in the computations, such as those illustrated in figure 9 the effect of the wall boundary conditions on the particle phase is localized, and the global features of the flow remain for any choice of such conditions. This aspect was confirmed through numerical experimentation by performing computations analogous to those presented in figure 9 with a variety of boundary conditions imposed on the particulate phase at  $\zeta = 0$ .

### B.3. $\mathcal{K} > 0$

The structure of the small-time solution in this case proceeds as above, but with a marked difference: the absence of a front, a fact that is apparent from the discussion in §4.3.2 (and also because in this case  $\delta$ , as defined above, will be negative). In fact, from (4.35) we recall that  $w_p$  is given uniformly in space and time by  $(-\gamma \mathcal{K}/\beta)$ . Therefore, equations (B 9) and (B 10) are in this case too the leading-order terms in the time series, and are valid down to the wall. Thus, we see that the particle slip begins at small time; evaluating (B 9) and (B 10) at the wall gives

$$\left. \begin{aligned} u_p &= \frac{4}{15} u'_0(0) t^{5/2} + O(t^{7/2}), \\ v_p &= \frac{\beta}{\gamma} t + O(t^2) \quad \text{at } \zeta = 0. \end{aligned} \right\}$$

### REFERENCES

- ALLAHAM, A. A. & PEDDIESON, JR., J. 1993 The flow induced by a rotating disk in a particulate suspension. *Intl J. Engng Sci.* **31**, 1025.
- BENTON, E. R. & CLARK, A. 1974 Spin-up. *Annu. Rev. Fluid Mech.* **6**, 257.
- DREW, D. A. 1983 Mathematical modeling of two-phase flow. *Annu. Rev. Fluid Mech.* **15**, 261.
- DUCK, P. W. & FOSTER, M. R. 2001 Spin-up of homogeneous and stratified fluids. *Annu. Rev. Fluid Mech.* **33**, 231.
- HERNÁNDEZ, J. A. 2001 Instabilities induced by concentration gradients in dusty gases. *J. Fluid Mech.* **435**, 247.
- ISHII, M. 1975 *Thermo-fluid Dynamic Theory of Two-phase Flow*. Eyrolles, Paris.
- JACKSON, R. 1996 Locally averaged equations of motion for a mixture of identical spherical particles in a Newtonian fluid. *Chem. Engng Sci.* **52**, 2457.
- LI, A. & AHMADI, G. 1993 Deposition of aerosols on surfaces in a turbulent channel flow. *Intl J. Engng Sci.* **31**, 435.
- MARBLE, F. E. 1970 Dynamics of dusty gases. *Annu. Rev. Fluid Mech.* **2**, 397.
- MANG, J., UNGARISH, M. & SCHAFLINGER, U. 2001 Gravitational-centrifugal separation in an axisymmetric source-sink flow with a free surface. *Intl J. Multiphase Flow* **27**, 197.
- OSIPTSOV, A. N. 1997 Mathematical modeling of dusty-gas boundary layers. *Appl. Mech. Rev.* **50**, 6, 357.

- RESNICK, R. I. 1990 Numerical analysis of two-phase rotating flows. M.Sc. Thesis, Technion, Israel Inst. Tech.
- SAFFMAN, P. G. 1965 The lift of a small sphere in a slow shear flow. *J. Fluid Mech.* **22**, 385 (and Corrigendum, 1968, **31**, 624).
- SLATER, A. S. & YOUNG, J. B. 2001 The calculation of inertial particle transport in dilute gas-particle flows. *Intl J. Multiphase Flow* **27**, 61.
- UNGARISH, M. 1993 *Hydrodynamics of Suspensions*. Springer.
- UNGARISH, M. & GREENSPAN, H. P. 1983 On two-phase flow in a rotating boundary layer. *Stud. Appl. Maths* **69**, 145 (referred to herein as UG).
- ZHANG, D. Z. & PROSPERETTI, A. 1997 Momentum and energy equations for disperse two-phase flows and their closure for dilute suspensions. *Intl. J. Multiphase Flow* **23**, 3, 425.
- ZUNG, L. B. 1969 Flow induced in fluid-particle suspension by an infinite rotating disk. *Phys. Fluids* **12**, 18.